PHYSICAL REVIEW E **80**, 030904(R) (2009)

Free-running period of neurons in the suprachiasmatic nucleus: Its dependence on the distribution of neuronal coupling strengths

Changgui Gu, Jianxiong Wang, and Zonghua Liu*
Institute of Theoretical Physics and Department of Physics, East China Normal University, Shanghai 200062, China
(Received 9 July 2009; published 30 September 2009)

The suprachiasmatic nucleus (SCN) pacemaker shows a free-running period ranging from 20 to 28 h for different species, which was usually explained from the angle of coupling strength. Based on the assumption of nonidentical coupling strengths in SCN, we find an alternative mechanism that the diversity of free-running period can be also caused by the distribution of coupling strengths. The free-running period is proportional to the average coupling strength and inverse proportional to the dispersion of couplings. Moreover, we present an analytic phase model to confirm our finding, which shows a solid foundation of our finding and opens a window to study the collective behaviors of SCN oscillators.

DOI: 10.1103/PhysRevE.80.030904 PACS number(s): 87.18.Sn, 05.45.Xt

It is well known that almost all the plants and animals have rhythms which can be detected by five senses: sight, sound, touch, smell, and taste [1]. Most of the rhythms are closely related to the 24 h circadian period of sunlight such as the insect emergence, roosters crowing, and sleep-waking behavior. A desire to understand the rhythms has motivated extensive experimental and theoretical works [1–6]. It is found that in the absence of daily light-dark cycle, the free-running periods are different for different species. For example, the free-running period is about 21.5 h in Neurospora, about 28 h in Phaseolus, close to 24.4 h in Drosophila, close to 25.6 h in Zebrafish, between 23.5 and 24.5 h for Bat, between 23.5 and 24 h for Squirrel, and 24.2 h for people living in carefully controlled lighting conditions [3–6]. Thus, the free-running period differs from 24 h for most species and scatters roughly in the range between 20 and 28 h. Based on the population genetics models, Daido suggested that the reason for different free-running periods is because it is beneficial for species [7]. However, it remains unclear how the difference of free-running periods show up.

The mammal's rhythm is controlled by the suprachiasmatic nucleus (SCN) of the hypothalamus, i.e., a central circadian clock in mammals, and has been well studied [8–15]. The SCN is composed of about 20 000 neurons and can be anatomically and functionally divided into two regions: ventrolateral SCN or "core" and dorsomedial SCN or "shell" with the shell largely surrounding the core. The SCN receives light signals from the retina and then controls circadian rhythms in peripheral tissues and behavioral activity. The shell oscillators are entrained by the core ones to form a single integrated oscillator. The shell has a shorter period than the core.

There are a lot of neurons in both the core and shell regions. The neurons in the two regions would synchronize each other to form a single integrated oscillator. When the daily light-dark cycle is added, all the neurons are entrained to the 24 h day. A key important question here is how such a regulatory network of heterogeneous circadian oscillators achieves a synchronous and coherent output rhythm [2,7,16–18]. For answering this question, several models have been presented [2,16,19–21], which are based on the Goodwin oscillator with three variables [22], i.e., a negative transcription-translation feedback loop. For example, Gonze *et al.* considered a global coupling strength depending on the concentration of neurotransmitter into the Goodwin oscillator and made them be influenced under a mean field [2,16]. Locke *et al.* modified the system to coupled damped oscillators [17]. Other closely related models were presented for the circadian clock in Neurospora [19–21].

It has been pointed out that the individual neurons in SCN are not identical with the same period but exhibit circadian firing rhythms with different periods ranging from 20 to 28 h and distributed normally [9,10,23]. To consider this fact, a factor τ_0/τ_i was multiplied into the modified Goodwin model to represent the distinct periods of individual oscillators [2,4,16,17]. It was also suggested that for a specific species, the strength of neurotransmitter feedback appears to vary from neuron to neuron in SCN [17]. However, the influence from nonidentical coupling strengths in individual neurons has not been discussed so far. In this Rapid Communication, we will consider the case with distributed coupling strengths to replace the previous constant coupling. We find that the distribution can significantly influence the output period of coupled neurons, which shows an alternative mechanism for the scattering periods of various species and sheds light on the mechanism of the free-running period of SCN clock. Furthermore, we present an analytic phase model to show a solid foundation of our finding and open a window to study the collective behaviors of SCN oscillators.

The coupled Goodwin oscillators can be represented as follows [2,16,17]:

$$\dot{x}_i = \alpha_1 \frac{k_1^n}{k_1^n + z_i^n} - \alpha_2 \frac{x_i}{k_2 + x_i} + \alpha_c \frac{gF}{k_c + gF} + L,$$

$$\dot{y}_i = k_3 x_i - \alpha_4 \frac{y_i}{k_4 + y_i},$$

$$\dot{z}_i = k_5 y_i - \alpha_6 \frac{z_i}{k_6 + z_i},$$

*zhliu@phy.ecnu.edu.cn

$$\dot{V}_i = k_7 x_i - \alpha_8 \frac{V_i}{k_8 + V_i}, \quad i = 1,2, \ldots, N, \tag{1}$$

where $F=\frac{1}{N}\Sigma_{i=1}^{N} V_i, x_i, y_i$, z_i constitute a negative feedback loop in the clock cell $-i$, x represents a clock gene messenger Ribonucleic Acid (mRNA) , y represents a clock protein, and z represents a transcriptional inhibitor. V is a neuropeptide induced by the activation of the clock gene x and can synchronize clock cells. The intercellular coupling is implemented through the global neurotransmitter F, which acts as a mean field. The coupling strength g describes the sensitivity of the individual circadian oscillator to the neurotransmitter and L denotes the light. Following Ref. [17] we take the parameters as $\alpha_1=6.8355$ nM/h, $k_1=2.7266$ nM, $n=5.6645$, $\alpha_2=8.4297$ nM/h, $k_2=0.2910$ nM, $k_3=0.1177$/h, $\alpha_4=1.0841$ nM/h, $k_4=8.1343$ nM, $k_5=0.3352$/h, $\alpha_6=4.6645$ nM/h, $k_6=9.9849$ nM, $k_7=0.2282$/h, $\alpha_8=3.5216$ nM/h, $k_8=7.4519$ nM, $\alpha_c=6.7924$ nM/h, and $k_c=4.8283$ nM. Different periods of individual oscillators are implemented by rescaling rate constants, i.e., by dividing $\alpha_1, \alpha_2, k_3, \alpha_4, k_5, \alpha_6, k_7$, and α_8 by a scaling factor τ_i, $i=1, \ldots, N$. The values of τ_i are taking randomly from a normal distribution [2,4,16,17].

We are here interested in its free-running period. Thus, we consider the case of absence of light, $L=0$. Considering that the strength of neurotransmitter feedback appears to vary from neuron to neuron [17], we use g_i to reflect this feature and let it satisfy a normal distribution with average $\langle g \rangle$ and variance σ. Therefore, the first equation of Eq. (1) can be rewritten as

$$\dot{x}_i = \alpha_1 \frac{k_1^n}{k_1^n + z_i^n} - \alpha_2 \frac{x_i}{k_2 + x_i} + \alpha_c \frac{g_i F}{k_c + g_i F}, \tag{2}$$

and the other equations in Eq. (1) remain unchanged. Our numerical simulation shows that the coupled system (2) will be in an oscillatory state only when the average coupling strength is larger than a minimum $\langle g \rangle_m$ and in a fixed point otherwise. For investigating the influence of the distribution of g_i we first focus on the case of $\tau_i=1$ for all the oscillators, i.e., identical oscillators with different g_i. We find that the results obtained from the constant $\tau_i=1$ also work for the case with distributed τ_i.

The overall degree of synchrony over a specific time period can be measured by an order parameter

$$R = \frac{\langle F^2 \rangle - \langle F \rangle^2}{\frac{1}{N}\sum_{i=1}^{N} (\langle V_i^2 \rangle - \langle V_i \rangle^2)}, \tag{3}$$

where $\langle . \rangle$ denotes average over time [16]. This parameter measures the distribution of phases of the oscillators. R will be 0 for unsynchronized oscillators and 1 for perfect synchronization. In the synchronized state, all the oscillatory V_i has the same period T. For a given distribution of g_i, part of g_i will be greater than the average $\langle g \rangle$ and the other will be less than $\langle g \rangle$. The final status of the coupled oscillators is determined by the competition between the oscillators with $g_i > \langle g \rangle$ and that with $g_i < \langle g \rangle$. The system will show an oscillatory behavior when $\langle g \rangle > \langle g \rangle_m$ and gradually decay to a fixed point otherwise. We are interested in the region of oscillation. Figure 1(a) shows how R changes with $\langle g \rangle$ for $\sigma=0$, 0.05, 0.1, 0.15, 0.2, 0.25, and 0.3, respectively, where the left ending point on each curve denotes the $\langle g \rangle_m$. From Fig. 1(a) it is easy to see that all the R are almost larger than 0.8, indicating that once the coupled oscillators are in the oscillatory state, they are approximately synchronized. On the other hand, Fig. 1(a) tells us that $\langle g \rangle_m$ is different for different σ. Figure 1(b) shows how $\langle g \rangle_m$ changes with σ. From Fig. 1(b) we see that $\langle g \rangle_m$ is linearly proportional to σ, indicating that large σ needs larger $\langle g \rangle_m$ to make the system be oscillatory.

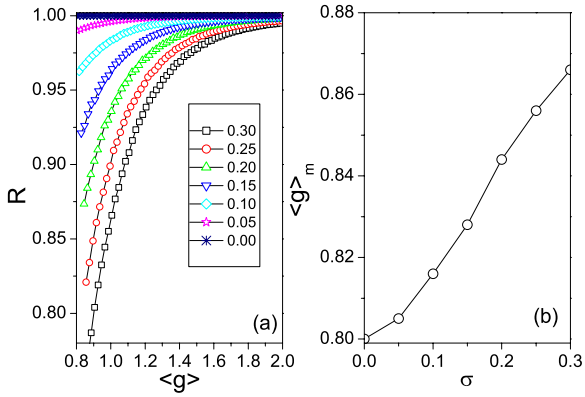

FIG. 1. (Color online) (a) The order parameter R versus the average coupling strength $\langle g \rangle$ for different dispersions $\sigma=0$, 0.05, 0.1, 0.15, 0.2, 0.25, and 0.3, respectively. (b) The minimum coupling strength to sustain oscillation, $\langle g \rangle_m$, versus σ. The number of coupled oscillators is $N=1001$.

For the synchronized oscillators, they will have an output period T, i.e., the free-running period. We find that T generally increases with $\langle g \rangle$, which is consistent with the results in Refs. [2,16]. Figure 2(a) shows how T changes with $\langle g \rangle$ for different σ. Obviously, T is not sensitive to σ for larger $\langle g \rangle$ but very sensitive to σ for smaller $\langle g \rangle$. This is an interesting result as it shows that the output period depends also on the dispersion σ. Figure 2(b) shows how T changes with the

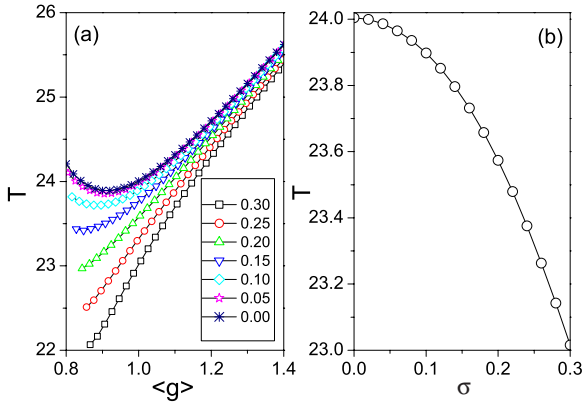

FIG. 2. (Color online) (a) Output period versus the average coupling strength $\langle g \rangle$ for different dispersions $\sigma=0$, 0.05, 0.1, 0.15, 0.2, 0.25, and 0.3, respectively. (b) Output period versus the dispersion σ for $\langle g \rangle=1$. The number of coupled oscillators is $N=1001$.

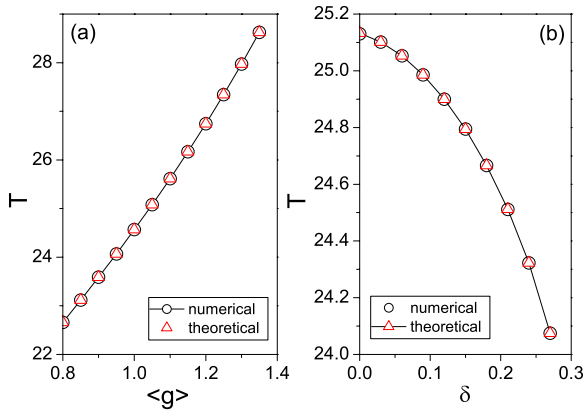

FIG. 3. (Color online) Dependence of output period on the average coupling strength $\langle g\rangle$ in (a) and the dispersion σ in (b) where the parameters are $N=1001$, $\omega_0=0.35$, $b=0.1$, the triangles and circles represent the theoretical and numerical results, respectively, and $\sigma=0.2$ in (a) and $\langle g\rangle=1$ in (b).

dispersion σ for fixed $\langle g\rangle=1$. It is easy to see that T decreases monotonously with σ, indicating that *the distribution of coupling strengths will influence the output period*. We have observed the similar result for the case of uniform random distribution of g_i. Thus, this result is robust to the distributions and may be significant in understanding the diversity of free-running periods. That is, the diversity of free-running periods may also come from the different distributions of coupling strengths in different species. We expect this prediction will be confirmed by experiments in the near future.

To explain our finding theoretically, we present an analytic phase model as follows. From Fig. 2(a) we see that the period T is approximately proportional to $\langle g\rangle$, implying that larger g_i corresponds to larger T or equivalently small frequency ω_i for individual oscillators. This observation suggests us that the intrinsic frequency of the ith oscillator can be assumed as $\omega_i=\omega_0-bg_i$ with constants ω_0 and b. To consider the dispersion of coupling, we assume that the number of oscillators with the same coupling g_i satisfy a normal distribution with average $\langle g\rangle$ and standard variation σ. Thus, we obtain a phase model

$$\dot{\theta}_i = \omega_0 - bg_i + \frac{g_i}{N}\sum_{i=1}^{N} \sin(\theta_j - \theta_i), \tag{4}$$

with $1\le i,j\le N$.

When the coupled oscillators are synchronized, they will have a common frequency Ω. Letting $t=0$ be the time for the oscillators to be synchronized, the solution of Eq. (4) can be expressed as

$$\theta_i = \Omega t + \theta_{i0}, \tag{5}$$

where θ_{i0} is the phase of the oscillator-i right before synchronization. Substituting Eq. (5) into Eq. (4) we find that the coupling term $g_i/N\Sigma_{i=1}^{N}\sin(\theta_j-\theta_i)$ becomes a constant $g_i/N\Sigma_{i=1}^{N}\sin(\theta_{j0}-\theta_{i0})$, i.e., independent of time. Thus, we may assume $\Sigma_{i=1}^{N}\sin(\theta_j-\theta_i)$ depend only on the coupling g_i and can be denoted as $f(g_i)$. Substituting it into Eq. (4) and considering Eq. (5) we have

$$\Omega = \omega_0 - bg_i + \frac{g_i}{N}f(g_i). \tag{6}$$

It is easy to see that $f(g_i)/N=b+(\Omega-\omega_0)/g_i\equiv b+c/g_i$. Considering the condition $\Sigma_{i=1}^{N}\frac{1}{N}\Sigma_{j=1}^{N}\sin(\theta_j-\theta_i)=0$ we obtain $\Sigma_{i=1}^{N}f(g_i)/N=\Sigma_{i=1}^{N}(b+c/g_i)=0$, which gives $c=-Nb/\Sigma_{i=1}^{N}1/g_i=-b/\langle 1/g\rangle$. Thus, we have

$$\Omega = \omega_0 - b/\left\langle\frac{1}{g}\right\rangle. \tag{7}$$

As the number of g_i satisfies the normal distribution, in the limit of $N\to\infty$ we have

$$\begin{aligned}\left\langle\frac{1}{g}\right\rangle &= \int_0^\infty \frac{1}{g}\frac{1}{\sqrt{2\pi}\sigma}e^{-(g-\langle g\rangle)^2/2\sigma^2}dg \\ &\approx \frac{1}{2\sqrt{\pi}}\int_{x_0}^{0}\frac{-1}{\sqrt{x}(\langle g\rangle-\sqrt{2\sigma^2 x})}e^{-x}dx \\ &\quad+\frac{1}{2\sqrt{\pi}}\int_0^{x_0}\frac{1}{\sqrt{x}(\langle g\rangle+\sqrt{2\sigma^2 x})}e^{-x}dx \\ &= \frac{1}{\sqrt{\pi}}\int_0^{x_0}\frac{\langle g\rangle}{\sqrt{x}(\langle g\rangle^2-2\sigma^2 x)}e^{-x}dx,\end{aligned} \tag{8}$$

where $x_0=\langle g\rangle^2/2\sigma^2$. Obviously, $\langle\frac{1}{g}\rangle$ decreases with the increase in $\langle g\rangle$ but increases with the increase in σ. Hence, the output period

$$T = \frac{2\pi}{\Omega} = \frac{2\pi}{\omega_0 - b/\left\langle\frac{1}{g}\right\rangle} \tag{9}$$

will increase with $\langle g\rangle$ but decreases with the increase in σ. Our numerical simulations from Eq. (4) have confirmed this prediction [Eq. (9)]. Figure 3 shows the results where the parameters are $N=1001$, $\omega_0=0.35$, $b=0.1$, the "triangles" and "circles" represent the theoretical and numerical results, respectively, and $\sigma=0.2$ in (a) and $\langle g\rangle=1$ in (b). From Fig. 3 it is easy to see that the numerical simulations perfectly confirm the theoretical results.

Except the Gaussian distribution, we find that similar results can be also obtained by other distributions of g_i such as the uniform random distribution. For this distribution, we may rearrange g_i by ascending order and let $g_N-g_1=N\varepsilon\equiv\delta$, i.e., $g_i=g_1+i\varepsilon$, with ε being the interval of two consecutive g_i and δ being the total width of the coupling strength. In the limit of $N\to\infty$, the factor $\langle 1/g\rangle$ in Eq. (7) can be calculated as follows:

$$\begin{aligned}\left\langle\frac{1}{g}\right\rangle &= \int_0^1 \frac{1}{g_1+N\varepsilon x}dx = \frac{1}{N\varepsilon}\ln\frac{g_1+N\epsilon}{g_1} \\ &= \frac{1}{\delta}\ln\left(1+\frac{\delta}{\langle g\rangle-\delta/2}\right).\end{aligned} \tag{10}$$

Thus, by Eq. (7) we obtain the output period

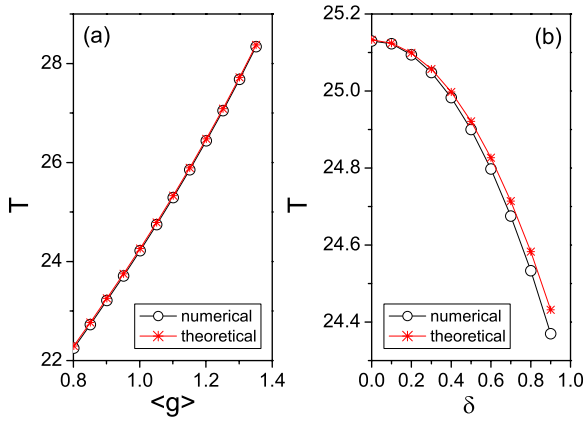

FIG. 4. (Color online) Dependence of output period on the average coupling strength $\langle g \rangle$ in (a) and the width of distribution δ in (b) where the parameters are $N=1001$, $\omega_0=0.35$, $b=0.1$ the asterisks and circles"\ represent the theoretical and numerical results, respectively, and $\delta=1$ in (a) and $\langle g \rangle=1$ in (b).

$$T = \frac{2\pi}{\omega_0 - b\delta/\ln\left(1 + \frac{\delta}{\langle g \rangle - \delta/2}\right)}. \tag{11}$$

From Eq. (11) it is easy to see that T will increase with $\langle g \rangle$ for fixed δ. For finding the relationship between T and δ, we may let $\ln(1+\delta/(\langle g \rangle - \delta/2)) \approx \delta/(\langle g \rangle - \delta/2)$ and then substitute it into Eq. (11). We find that T decreases with the increase in δ. Figure 4 shows the numerical simulations of the uniform random distribution where the parameters the "asterisks" and circles represent the results from Eqs. (4) and (11), respectively, and $\delta=1$ in (a) and $\langle g \rangle=1$ in (b). Obviously, the numerical simulations in both Figs. 4(a) and 4(b) are consistent with the theoretical prediction [Eq. (11)].

Comparing Fig. 4 with Fig. 3 we see that they are qualitatively similar, indicating that the phenomenon of dispersion reducing output period are independent of the specific distributions. We have also made numerical simulations on the case of nonidentical τ_i such as a Poisson distribution of τ_i and found a similar phenomenon. Therefore, the dispersion reducing output period is probably a characteristic feature of the SCN oscillators and might have significant contribution to the diversity of free-running periods in different species.

The diversity of free-running periods is a fundamental problem in biological rhythms. Many efforts have been paid to this topic, which are mainly focused on the aspect of experiments. Based on a mass of experimental data, a basic task is to form some theoretical models to reveal the underlying mechanism. Our phase model of SCN oscillators is nothing but one approach to implement the task. A characteristic feature of our model is that the intrinsic frequency is related to the coupling strength.

In conclusions, we have further modified the Goodwin model to include the feature of nonidentical coupling strengths of individual oscillators in SCN, which is based on the observation that the strength of neurotransmitter feedback appears to vary from neuron to neuron. For emphasizing on the contribution of distribution, we have ignored the influence from the aspects of different kinetic parameters and molecular mechanisms from one organism to another and also the different molecules of intercellular coupling. We find that for the cases of both identical and nonidentical oscillators, the free-running period depends on the dispersion of coupling strengths and decrease with the increase in dispersion. An analytic phase model is presented to reveal the mechanism of our finding, which provides insight to the diversity of free-running periods of SCN clock.

This work was supported by the NNSF of China under Grants No. 10975053 and No. 10635040 and by National Basic Research Program of China (973 Program) under Grant No. 2007CB814800.

[1] W. L. Koukkari and R. B. Sothern, *Introducing Biological Rhythms* (Springer, New York, 2006).
[2] S. Bernard, D. Gonze, B. Cajavec, H. Herzel, and A. Kramer, PLOS Comput. Biol. **3**, e68 (2007).
[3] A. Ahlgren and F. Halberg, *Cycles of Nature: An Introduction to Biological Rhythms* (National Science Teachers Association, Washington, D.C., 1990).
[4] G. Kurosawa and A. Goldbeter, J. Theor. Biol. **242**, 478 (2006).
[5] C. A. Czeisler *et al.*, Science **284**, 2177 (1999).
[6] M. R. Smith, H. J. Burgess, L. F. Fogg, and C. I. Eastman, PLoS ONE **4**, e6014 (2009).
[7] H. Daido, Phys. Rev. Lett. **87**, 048101 (2001).
[8] R. Y. Moore, J. C. Speh, and R. K. Leak, Cell Tissue Res. **309**, 89 (2002).
[9] D. K. Welsh, D. E. Logothetis, M. Meister, and S. M. Reppert, Neuron **14**, 697 (1995).
[10] S. Honma, W. Nakamura, T. Shirakawa, and K. Honma, Neurosci. Lett. **358**, 173 (2004).
[11] M. H. Hastings and E. D. Herzog, J. Biol. Rhythms **19**, 400 (2004).
[12] T. Kalamatianos, I. Kallo, H. D. Piggins, and C. W. Coen, J. Comp. Neurol. **475**, 19 (2004).
[13] T. Noguchi and K. Watanabe, Brain Res. **1239**, 119 (2008).
[14] H. Albus, M. J. Vansteensel, S. Michel, G. D. Block, and J. H. Meijer, Curr. Biol. **15**, 886 (2005).
[15] L. P. Shearman, M. J. Zylka, D. R. Weaver, L. F. Kolakowski, Jr., and S. M. Reppert, Neuron **19**, 1261 (1997).
[16] D. Gonze, S. Bernard, C. Waltermann, A. Kramer, and H. Herzel, Biophys. J. **89**, 120 (2005).
[17] J. C. W. Locke, P. O. Westermark, A. Kramer, and H. Herzel, BMC Syst. Biol. **2**, 22 (2008).
[18] Y. Li, J. Zhang, and Z. Liu, Int. J. Nonlinear Sci. **1**, 131 (2006).
[19] J. C. Leloup, D. Gonze, and A. Goldbeter, J. Biol. Rhythms **14**, 433 (1999).
[20] P. Ruoff and L. Rensing, J. Theor. Biol. **179**, 275 (1996).
[21] P. Ruoff, M. Vinsjevik, C. Monnerjahn, and L. Rensing, J. Theor. Biol. **209**, 29 (2001).
[22] B. C. Goodwin, Adv. Enzyme Regul. **3**, 425 (1965).
[23] T. Noguchi, K. Watanabe, A. Ogura, and S. Yamaoka, Eur. J. Neurosci. **20**, 3199 (2004).